

Qualitative Experiment with Arc Discharges on Negatively Biased Solar Cells

Hitoshi Kuninaka*

Institute of Space and Astronautical Science, Yoshinodai, Sagami-hara, Kanagawa, Japan

A high-voltage solar array, which can generate and transmit electrical power efficiently, may suffer serious degradation from arc discharges on negatively biased portions of the solar array. A qualitative experiment using heat-proof materials, which are different from those commonly used on solar cells, was conducted under conditions that eliminated the chamber wall effects. The experiment showed that there was a dependence of the discharge on the substratum temperature, which implies that surface adsorption of residual gas plays an important role in the initiation of the arc discharge.

Introduction

POWER requirements in space have increased dramatically since the first flights in the 1950s from a few watts to the multikilowatt systems of the 1970s and 1980s. They will increase more and more in the era of space industrialization. Photovoltaic power generation has been one of the most reliable power supplies in space since the beginning of the space era and will likely keep that position in the future. However, in order to adapt to the growth in power requirements, the following advancements in photovoltaic power generation are necessary: 1) the development of thin and highly efficient solar cells; 2) the development of flexible lightweight structures for the solar array substrate; and 3) the creation of the technology for power generation and transmission at high voltage. The third factor, which is familiar for the ground-based power systems, allows reduction in the weight of the wire harness and eliminates the Joule losses in it so as to improve the system efficiency.

The higher the voltage becomes, however, the more severe the impact arising from the spacecraft interactions with the space plasma.¹ Low Earth orbit (LEO) will be particularly severe for high-voltage solar arrays (HVSA) as the interconnectors between the solar cells are typically exposed directly to the ionospheric plasma. The following issues resulting from the HVSA system must be resolved: 1) local breakdown of the solar cells; 2) power loss due to parasitic plasma current; 3) ion-induced drag; and 4) material degradation by sputtering. The first item is thought to be the most severe problem for the HVSA system because the occasional discharge not only damages the solar cell itself but also causes electromagnetic interference and conductive noise in the power line. Flight tests^{2,3} and ground experiments^{4,5} have demonstrated that environmentally induced discharges occur on negatively biased solar cells. Although theories⁶⁻⁸ on the cause of these discharges have appeared, no theory currently exists that completely explains environmentally induced discharges on negatively biased solar cells. Current experimental efforts seek redundant ways to overcome the plasma interactions of the HVSA. The development of the wrap-through type solar cell,⁹ which is insulated entirely from the environment, is one of the solutions.

References 6 and 8 suggest that the arc discharge is initialized by enhanced electron emission from the negatively biased surface and propagates in the gas produced from a surface ad-

sorption layer by electron-stimulated desorption (ESD). Parks et al.⁷ suggest that enhanced electron emission occurs from a containment layer, not identified, on the solar cell interconnectors. It is questionable if such a thick contaminant layer can survive repetitive arc discharges or primary ion collision.⁵

In previous work, the author carried out a ground experiment¹⁰ that simulated ion collection by the HVSA from the ionospheric plasma and was modeled using a similarity law. The experiment determined the characteristics of the parasitic current, ion-induced drag, and material degradation by sputtering. The scale experiment had the advantage of allowing visualization of the interference phenomena caused by denser plasma than that in the ionosphere. This visualization of unknown phenomena is useful in identifying them. Such artificial situations can also be used to verify the hypotheses. The objectives of the present work are to study arc discharges on the negatively biased solar cells by a similar scale experiment and to provide an explanation of its causes.

Ground Experiments

The scale experiment, using a small-scale-model solar array, was developed to simulate ion collection by a large HVSA using a denser plasma¹⁰ than that in LEO. The small-scale experiment has the following advantages in comparison with a full-scale experiment on the ground:

- 1) A huge space chamber and ultrahigh plasma flow are unnecessary.
- 2) It is possible to produce uniform plasma flow over a miniature model.
- 3) Some phenomena can be visualized due to the dense plasma.
- 4) An experiment in an artificial test environment is useful in the verification of a hypothesis.

Associated with the application of the scale experiment to an arc discharge, the first, third, and fourth items assist in the construction and the verification of a possible explanation of the discharge. We can reduce the interference by the chamber wall in the ground experiment because the dense plasma electrically shields the solar cell model from the wall. As mentioned in the previous section, the amount of gas adsorbed on the solar cell surface might affect the arc discharge. The

Table 1 Experimental conditions in laboratory

Electron temperature, eV	2.2
Plasma density, cm ⁻³	2 × 10 ⁹
Ion beam energy, eV	40
Magnetic field, g	4
Ion mass number	40
Dominant ion species	Ar ⁺
Neutral density, cm ⁻³	7 × 10 ¹²

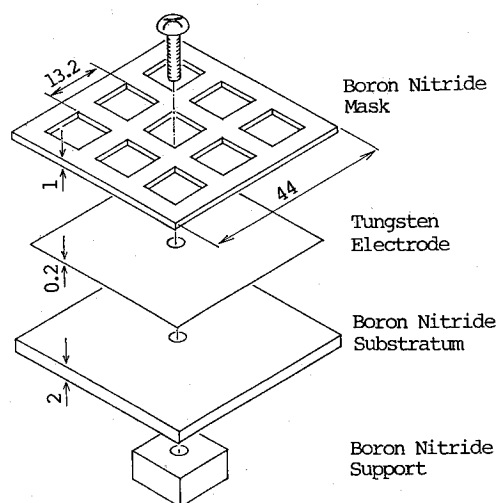


Fig. 1 Structure of masked model.

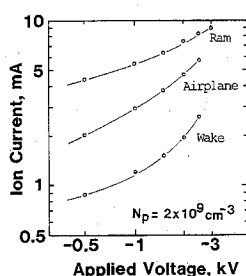


Fig. 2 Ion current collected by masked model vs bias voltage. Parameter is relative attitude of masked model to plasma flow.

technique of thermal desorption spectrum (TDS) suggests that the amount of adsorption is controlled by the temperature of the adsorbent.¹¹ Such a high temperature over 200°C cannot apply to real solar cells because it would alter the material properties of the organic materials used in the solar cells. An experimental simulation using heat-proof materials was conducted.

Vacuum System and Plasma Source

All simulations were carried out in a stainless-steel space chamber, which is 2.8 m in length and 1.5 m in diameter. The plasma flow was generated by a steady-state Hall-type accelerator using argon with a 2×10^{-4} Torr back pressure. The plasma parameters were measured by a Langmuir probe, a retarding potential analyzer, a time-of-flight method, an optical multichannel analyzer, and a Hall sensor. The properties of the plasma produced at 17 cm downstream from the exit of the accelerator are listed in Table 1.

Solar-Cell Model

The solar cell was simulated by a 4.4-cm length square of tungsten plate, a substratum, and a mask as illustrated in Fig. 1. The substratum and the mask made of boron nitride were insulators. The area of the exposed electrode was 7.0 cm². The side surface of the model was coated with an inorganic and nonconductive paint so as not to expose the electrode. To control the temperature of the solar-cell model, a heater and a thermocouple were attached to the back of the substratum. The model without the mask was also tested.

The orientations of the model electrode surfaces directed upstream or downstream of the plasma flow are called "ram" and "wake" modes, respectively. The orientation in which the electrode surfaces are parallel to the plasma flow is called the "airplane" mode. The models were uniformly biased in the plasma to as low as -3 kV with reference to the ground by

use of a constant-voltage power supply. The circuit of the power supply did not contain a decoupling resistor limiting the discharge current. The discharge current was monitored by a shunt resistor of 0.5 Ω and by a digital memory with an input impedance of 20 pF and 1 M Ω .

Emissive Probe

Potential distributions around the models were measured by an emissive probe mounted on an X-Y table driven by a microcomputer. The probe was made of 0.2-mm-diam thoriated tungsten wire and heated by a 5-A current. The probe current was measured according to probe location at a constant potential in contrast to the ordinal method¹² of the emissive probe. A position where the emissive current drops suddenly to near zero is identified as having the same potential as that of the probe. Errors were ± 1 mm in location and ± 5 V in potential.

Experimental Results

Luminosity on Insulator Surface

When biased negatively in the plasma, the masked model collected ion current depending on the bias voltage and the orientation to the plasma flow as shown in Fig. 2. Each surface of the tungsten electrode glowed as shown in Fig. 3.¹⁰ Below about -1-kV potential, luminosity in the form of tongue was observed on the boron nitride surface of the masked model. It appeared to be in steady state and the magnitude was dependent on the bias voltage and the model temperature. Figure 3 shows the dependence of the surface luminosity on the model temperature. Below about 250°C the luminosity on the insulator was visible, but at higher temperatures it disappeared. When the model was cooled below 250°C, the luminosity on the insulator could be observed again.

Arc Discharge

The nonmasked model could be biased negatively to as much as -3 kV with no arcs. In contrast, frequent arc discharges occurred on the masked model below about -1.5 kV. The discharge pulse typically has a peak current on the order of 10 A and was several microseconds in pulse width. The temperature dependence of the discharge frequency is shown in Fig. 4. A pulse over 10 A in peak current was regarded as a discharge in order to count arc discharges. After heating the model to a certain temperature and leaving it biased at -1.5

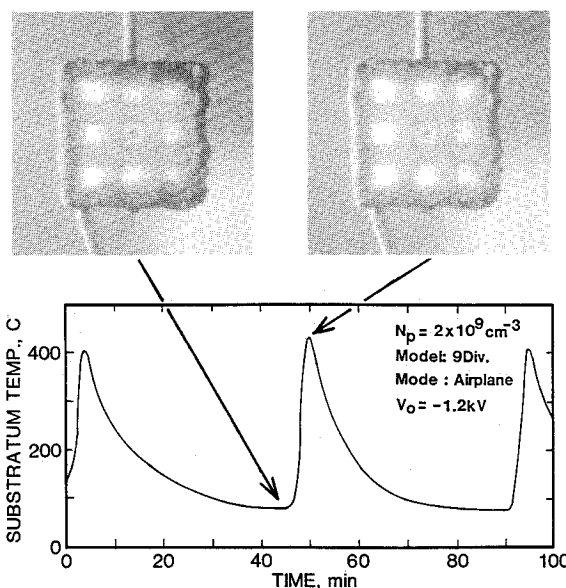


Fig. 3 Temperature dependence of luminosity on masked model insulator.

kV for over 10 min, discharges were observed to occur every few seconds. The discharge frequency decreased as temperature increased until it saturated at a constant value about 300°C.

Spatial Potential Distribution

Figures 5 and 6 represent the potential distributions around the models without and with the mask as measured by the emissive probe. Emissive-probe data were used to identify positions corresponding to -40 V, -300 V, and -400 V along the center cross section of the models. A detailed contour around the masked model is seen in Fig. 7 for a -1.8-kV-biased potential. Within the restrictions of the emissive probe, the spatial potential could only be measured at positions further apart than 2.3 mm from the model surface. It should be noted that the ion beam energy was 40 eV for this experimental arrangement. The cross bars in Figs. 5-7 represent the spatial error.

Discussion

Experimental Scaling

Figures 6 and 7 imply that a single sheath entirely covers the masked model. In the case of the real solar cell in LEO, a negatively biased surface is also separated electrically from the ionospheric plasma by the ion sheath¹³ because the length of the space charge sheath exceeds the distance between the interconnectors. The author previously presented a nondimensional perveance P to indicate the magnitude of the plasma interaction¹⁰:

$$P = \frac{L_A^2 j_i}{\epsilon V_0^{3/2}} \sqrt{\frac{M}{2e}}$$

where L_A , V_0 , j_i , M , e , and ϵ are characteristic length of solar array, bias voltage, ram ion current density, ion mass, electric

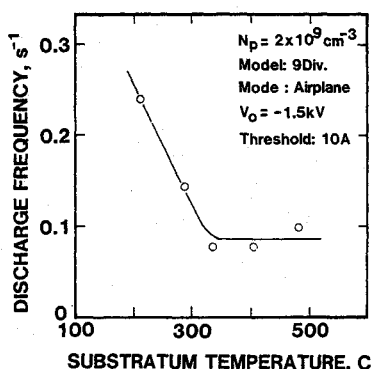


Fig. 4 Temperature dependence of discharge frequency.

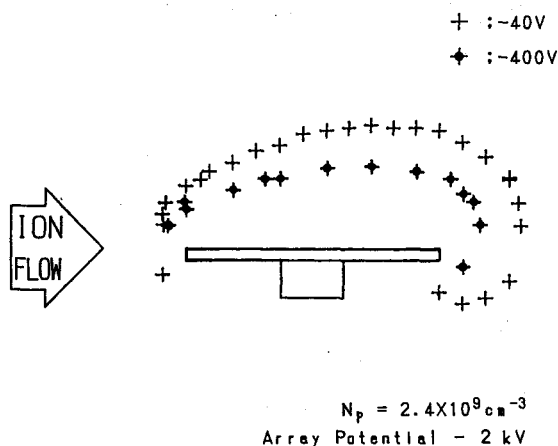


Fig. 5 Spatial potential distribution around nonmasked model.

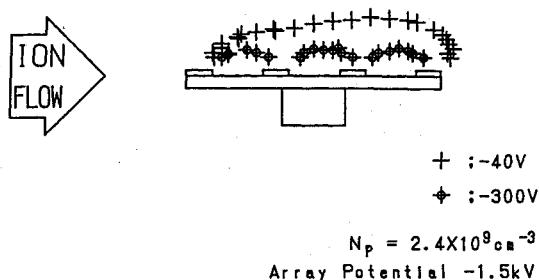


Fig. 6 Spatial potential distribution around masked model.

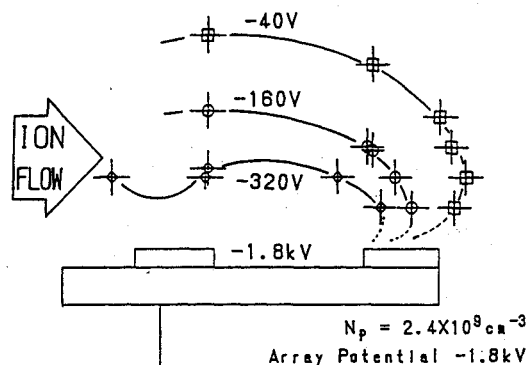


Fig. 7 Potential distribution in neighborhood of masked model surface.

charge, and permittivity, respectively. This parameter demonstrates a relation between a characteristic length of the HVSA and a length of the ion space charge sheath with the assumption of one-dimensional flow. When applied to a real solar cell in LEO, the nondimensional perveance is estimated to be 0.24, for ion mass number 16, ram ion flux of 2.4 mA/m², bias voltage of -160 V, and solar-cell length of 8 cm. The masked model, when biased to -3 kV, gives the same value as that of the real solar cell in the nondimensional perveance. The data are listed in Table 1 with an electrode interval of 13.2 mm for the masked model. This estimate suggests that the potential distribution formed around the mask is similar to the case of the real solar cell in LEO. Hence we believe that the scale experiment in the laboratory simulates the environment of the real negatively biased solar cell except for material effects. The experimental results, however, may not be quantitative owing to differences in the materials, environment, and the power supply, etc., between the simulation and a real solar cell in LEO. It is important to note that the scale experiment eliminates chamber-wall effects since the sheath dimension is much shorter than the chamber's because of the dense plasma. The observed phenomena are not caused by the presence of the chamber wall.

Electron Emission from Conductor Region

Since we have shown that the sheath covers the whole model, the electrons that can get to the insulator surface must be secondary electrons from the conductor. A plausible model for the surface luminosity is the result of an interaction between an adsorbate and secondary electrons from the conductor region. Because the amount of the adsorbate will be related to the temperature, this model can explain the dependence of the luminosity on the substratum temperature. This luminosity resembles the flight data on the spacecraft surface glow.¹⁴ The characteristic time T_a of the adsorption can be estimated as

$$T_a = Q/s n_n v_n$$

where Q , s , n_n , and v_n are amount of adsorption per unit area, sticking probability of the adsorbate, neutral particle

density, and velocity, respectively. Adsorption above room temperature is dominated by chemisorption for which the value of Q is limited by a monomolecular layer. In the scale experiment, the time T_a is on the order of 1 ms, where Q , s , n_n , and v_n are assumed to be $1 \times 10^{18} \text{ m}^{-2}$, 0.5 , $7 \times 10^{18} \text{ m}^{-3}$, and 300 m/s , respectively. Because the time T_a is much less than the characteristic time variation of the substratum temperature, the phenomenon in Fig. 3 can be assumed to be in quasiequilibrium. The saddle-shaped potential distribution,¹³ necessary to generate the electrons incident on the mask, could not be found in the space charge sheath because of the limited spatial resolution of the emissive probe as shown in Fig. 7. Only the secondary electrons emitted from the conductor region have enough energy to excite the adsorbed gas on the mask.¹³ Not only the conductor surface⁷ but also the boundary region between the electrode and the insulator mask are candidates for the origin of secondary electrons.

Adsorption and Arc Discharge

Surface discharges were observed only for the masked model. This suggests that the discharge depends on the surface configuration rather than the ambient plasma.

In the scale experiment, the discharge occurs even though the conductor surface of the masked model is kept clean by frequent high-energy collisions of the primary ions (that is, argon etching). In earlier work,¹⁰ a tungsten electrode was pitted after operation in this environment. A contaminant layer, which was suggested as the initiator of the discharge in Ref. 7, cannot survive for a long time. For example, a 1000-\AA -thick layer consisting of particles 3-\AA in diameter will be sputtered completely away on the order of 100 s for a -1.5-kV -biased masked model in the airplane mode for unity sputtering yield.

The absolute value of the discharge frequency measured in the scale experiment should not be compared with that of a real solar cell in LEO. However, the temperature dependence of the discharge frequency in Fig. 4 and of the surface luminosity in Fig. 3 implies the existence of adsorption. Desorption of adsorbate at low binding states leaving the remainder of the adsorbate with a high binding energy is thought to be the cause of the saturation of the discharge frequency above 300°C (see Fig. 4). The residual gas forms a monolayer on the surface by chemisorption. The high-energy ions incidence on the conductor destroys the monolayer as well as any contaminant layer. The monolayers on the mask and the insulator near the conductor can survive.

Concluding Remarks

The ground simulation of arc discharges using heat-resistive materials in a dense argon plasma was conducted. The scale experiment can eliminate interactions with the vacuum chamber wall because of the plasma shielding. The experiment suggested the following: 1) arc discharges occurred only on the surface of the masked model, 2) arcs occurred on the model with a clean conductor, 3) the frequency of discharges depended on the substratum temperature, and 4) surface luminosity was observed on the insulator mask. The fourth result suggests that electrons are incident from the conductor region onto the mask. The first and second results are inconsistent

with the theory that the arcs are initiated in a contaminant layer on the conductors as in Ref. 7. The third result suggests that surface adsorption of residual gas may play some role in the arc discharge. It is necessary to construct a new theory for the arc discharge integrating the effects of the surface gas adsorption/desorption and the secondary electrons. Further research using real solar cells is needed to reveal the mechanism of the arc discharge on the negatively biased solar cells.

Acknowledgments

The author expresses appreciation to Yukishige Nozaki for cooperation with the experiment and assistance with the fabrication of the experimental apparatus. Gratitude is also extended to Prof. Daniel E. Hastings for his valuable discussions.

References

- ¹Stevens, N. J., "Review of Interactions of Large Space Structures with the Environment," *Progress in Astronautics and Aeronautics*, Vol. 47, edited by Alan Rosen, AIAA, New York, 1975, p. 437.
- ²Grier, N. T., and Stevens, N. J., "Plasma Interaction Experiment (PIX) Flight Results," NASA CP-2071, 1978, p. 295.
- ³Grier, N. T., "Plasma Interaction Experiment II (PIX II): Laboratory and Flight Results," NASA CP-2359, 1983, p. 333.
- ⁴Snyder, D. B., "Discharges on a Negatively Biased Solar-Cell Array in a Charged-Particle Environment," NASA CP-2359, 1983, p. 379.
- ⁵Thiemann, H., and Bogus, K. P., "High-Voltage Solar-Cell Modules in Simulated Low-Earth-Orbit Plasma," *Journal of Spacecraft and Rockets*, Vol. 25, No. 4, 1988, pp. 278-285.
- ⁶Marque, J. P., "Surface Discharge on e-Irradiated Materials," IFAC Workshop, Electrostatic Charges and Discharges and Cosmic Ray Interaction in Satellites, Paris, France, 1986.
- ⁷Parks, D. E., Jongeward, G. A., Katz, I., and Davis, V. A., "Threshold-Determining Mechanisms for Discharges in High-Voltage Solar Arrays," *Journal of Spacecraft and Rockets*, Vol. 24, No. 4, 1987, pp. 367-371.
- ⁸Hastings, D. E., Weyl, G., Kaufman, D., and Green, D., "Threshold Voltage for Arcing on Negatively Biased Solar Arrays," *Journal of Spacecraft and Rockets* (to be published).
- ⁹Ralph, E. L., "Photovoltaic Space Power History and Perspective," *Space Power*, Vol. 8, Nos. 1/2, 1989, p. 3.
- ¹⁰Kuninaka, H., Nozaki, Y., Satori, S., and Kuriki, K., "Ground Studies of Ionospheric Plasma Interactions with a High-Voltage Solar Array," *Journal of Spacecraft and Rockets*, Vol. 27, No. 4, 1990, pp. 417-424.
- ¹¹Redhead, P. A., Hobson, J. P., and Kornelsen, E. V., *The Physical Basis of Ultrahigh Vacuum*, Chapman and Hall, London, 1968, Chap. 2.
- ¹²Chen, F. F., "Electric Probe," *Plasma Diagnostic Technique*, edited by R. N. Huddleston and S. L. Leonard, Academic, New York, 1965.
- ¹³Jongeward, G. A., Katz, I., Mandell, M. J., and Parks, D. E., "The Role of Unneutralized Surface Ions in Negative Potential Arcing," *IEEE Transactions on Nuclear Science*, Vol. NS-32, No. 6, 1985, p. 4087.
- ¹⁴Swenson, G. R., Mende, S. B., and Llewellyn, E. J., "The Effect of Temperature on Shuttle Glow," *Nature*, Vol. 323, No. 9, 1986, p. 519.

Henry B. Garrett
Associate Editor